Orbital angular momentum correlations of entangled paired photons

2009 J. Opt. A: Pure Appl. Opt. 11 094013

(http://iopscience.iop.org/1464-4258/11/9/094013)

J. Opt. A: Pure Appl. Opt. **11** (2009) 094013 (7pp) doi:10.1088/1464-4258/11/9/094013

Orbital angular momentum correlations of entangled paired photons

Clara I Osorio[1], **G Molina-Terriza**[1,2] **and Juan P Torres**[1,3]

[1] ICFO—Institut de Ciencies Fotoniques, Mediterranean Technology Park, 08860 Castelldefels (Barcelona), Spain
[2] ICREA—Institucio Catalana de Recerca i Estudis Avancats, 08010 Barcelona, Spain
[3] Department of Signal Theory and Communications, Universitat Politecnica de Catalunya, Jordi Girona 1-3, 08034 Barcelona, Spain

E-mail: clara.ines.osorio@icfo.es

Received 10 December 2008, accepted for publication 30 January 2009
Published 5 August 2009
Online at stacks.iop.org/JOptA/11/094013

Abstract
The generation of paired photons entangled in the spatial degree of freedom, i.e., in orbital angular momentum, offers a convenient physical resource to investigate the nature of entanglement in a multidimensional Hilbert space with controllable dimensionality. The two main physical processes that generate pairs of photons which show correlations in orbital angular momentum are (a) spontaneous parametric down-conversion (SPDC), and (b) Raman transitions induced in atomic ensembles. One question naturally arises: *what kinds of correlations exist between the orbital angular momentum of the generated photons*? The answer might be different if we consider the whole quantum state of the generated photons, i.e., all possible directions where the pairs of photons can be emitted, or if we consider only a small section of the full set of directions.

Keywords: orbital angular momentum, parametric down conversion, Raman transitions, quantum optics and entanglement

(Some figures in this article are in colour only in the electronic version)

1. Introduction

The orbital angular momentum (OAM) of entangled photons is increasingly being used as a resource for the implementation of quantum information algorithms that, either inherently live in a Hilbert space of dimensions higher than two (qudits), or exhibit enhanced efficiency in increasingly higher dimensions (see [1] and references therein). These include the demonstration of the violation of bipartite, three-dimensional Bell inequalities [2], the implementation of the so called *quantum coin tossing* protocol with qutrits [3], and the generation of quantum states in ultra-high-dimensional spaces [4].

1.1. Spontaneous parametric down-conversion

All of the experiments mentioned above use as the source for generating paired photons with entangled properties, spontaneous parametric down-conversion (SPDC). In this process, an intense beam pumps a nonlinear crystal, where with a low probability, a pair of lower frequency photons is generated (see figure 1). Photons are known to be emitted in cones whose shape depends on the phase matching conditions inside the nonlinear crystal. Most of the relevant experiments reported up to now make use of a small section of the full down-conversion cone. Different sections of the down-conversion cone can thus be explored by relocating the single-photon counting modules.

Several experiments [5–8] seem to support the validity of the selection rule $m_p = m_s + m_i$, where $m_p\hbar$ is the OAM per photon of the classical pump beam, and m_s and m_i are the winding numbers of the modes into which the quantum state of the signal and idler photons are projected, respectively. In other words, only signal and idler photons that fulfil the above-mentioned selection rule can be detected. Some other experiments, while not directly measuring the OAM of the down-converted photons, demonstrate the existence of ellipticity of the spatial waveform [9–11], which should make possible the detection of photons with $m_p \neq m_s + m_i$. Under some restrictive conditions, the selection rule $m_p = m_s + m_i$ can be derived from first principles [12–14], although, as will

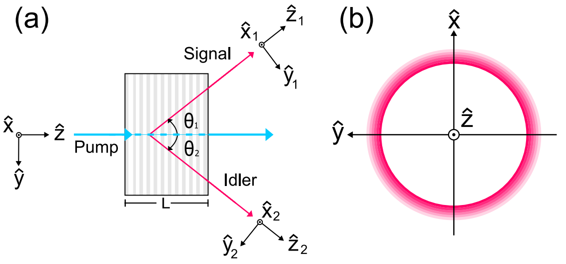

Figure 1. Schematic diagram of a non-collinear SPDC configuration. (a) Top view of the non-collinear configuration. (b) The down-conversion cone. The signal photon propagates along the $\hat{z}_1$ direction, and the idler photon along the $\hat{z}_2$ direction. The pump beam propagates along $\hat{z}$. The coordinates $(\hat{x}_j, \hat{y}_j)$ for $j = 1, 2$ designate the transverse planes corresponding to all of the interacting waves. $\theta_{1,2}$ are the angles of emission of the down-converted photons, and L is the length of the nonlinear crystal. The transverse dimensions of the crystal are assumed to be much bigger than the beam waist of the pump beam.

be shown below, the same rule addresses different physical quantities. Finally, the strength of the Poynting vector walk-off cannot be neglected when considering the OAM correlations of the down-converted photons [15–17], especially when using highly focused pump beams.

1.2. Raman transitions in atomic ensembles

Although SPDC is by far the most widely used source for generating entangled paired photons, in the last few years, another interesting scheme has been proposed that makes use of atomic ensembles to generate entangled pairs of photons. In this scheme, as shown in figure 2, a classical pump beam (the WRITE beam) impinges on an ensemble of N atoms, for instance, rubidium or cesium, and it induces the emission of, at most, a single photon *(Stokes photon)* from one of the atoms [18]. Such emission generates a collective atomic excitation that can be read by a control beam, which induces the emission of another photon *(anti-Stokes photon)* correlated with the Stokes photon. Quantum correlations mediated by the generation of a collective excitation in an ensemble of atoms have been observed in polarization [19], in the time–frequency [20], and in the orbital angular momentum (OAM) [21] degrees of freedom.

In a typical experimental configuration, the Stokes and anti-Stokes photons are detected in a small section of the full set of directions where the Stokes/anti-Stokes photons can be emitted [18, 22, 23]. In most cases, such detection modes are nearly collinear ($\sim 2°$–$3°$) with the direction of propagation of the counter-propagating pump and control beams [24]. But other situations can be considered as well, as in the case of transverse emitting configurations, where the Stokes/anti-Stokes photons propagate transversally to the pump/control beams [25].

Experiments reported up to now [21, 26] show that the selection rule $m_p - m_c = m_s - m_{as}$ is fulfilled, where $m_p\hbar$ and $m_c\hbar$ are the OAM per photon of the classical pump and control beams, and m_s and m_{as} are the winding numbers of the modes into which the quantum state of the Stokes and anti-Stokes photons are projected. Notwithstanding, when more general non-collinear configurations are considered [27], this selection rule seems to be violated.

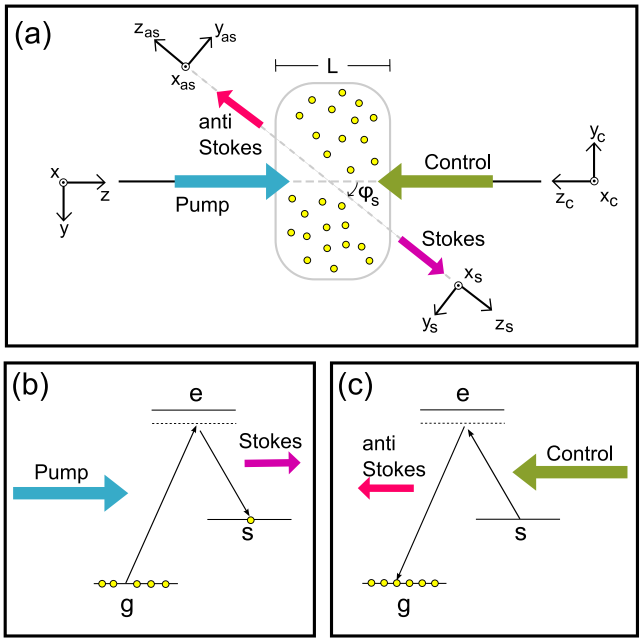

Figure 2. Configuration based on the use of Raman transitions induced in atomic ensembles. (a) Sketch of the geometric configuration. In a typical experimental configuration, the Stokes and anti-Stokes photons are detected in a small section of the full set of directions where the Stokes/anti-Stokes photons can be emitted. Two counter-propagating classical light beams are used to induce the emission of pairs of photons, the Stokes (s) and anti-Stokes (as) photons. (b) and (c) Level structure of the atoms that form the atomic cloud. The atoms have a Λ-type level configuration, with two hyperfine ground states, $|g\rangle$ and $|s\rangle$, and one excited state $|e\rangle$. All atoms are initially in the ground state $|g\rangle$.

Since many quantum information schemes are based on the existence of specific quantum correlations between pairs of photons, the characterization of such correlations is very important. The OAM correlations should be addressed in two complementary scenarios, so that in each scenario the sough-after OAM correlations can be different. In one scenario, the spatial properties of all of the pairs of photons generated are considered [12]. In this case, the OAM correlations can be modified by the presence of any effect that breaks the azimuthal symmetry around the pump beams that mediate the generation of the paired photons. In another scenario, which is relevant for current experimental applications, a small section of the full down-conversion cone is considered. Under this condition, the use of a non-collinear configuration, or the presence of spatial walk-off or any other symmetry-breaking perturbation, can greatly modify the OAM correlations observed. In particular, paired photons generated in different directions of emission show correspondingly different spatial quantum correlations and amount of entanglement.

This paper is divided into three sections. In section 2 we discuss how to describe the OAM of single-, and two-photon, quantum states. In section 3, we analyze the OAM correlations of the two-photon state, when all possible directions of emission of the generated photons are considered. Finally, in section 4, the OAM correlations of paired photons generated in collinear, or nearly collinear, configurations are discussed.

2. The orbital angular momentum of single and paired photons

2.1. Single photons

The spatial properties of a single-photon quantum state $|\Psi\rangle$ are described by a mode function Φ, so that

$$|\Psi\rangle = \int \mathrm{d}\mathbf{p}\, \Phi(\mathbf{p}) a^\dagger(\mathbf{p})|0\rangle \quad (1)$$

where $|0\rangle$ is the vacuum state, $\mathbf{p} = (p_x, p_y)$ is the transverse wavevector, and $a^\dagger(\mathbf{p})$ is the creation operator of one photon with transverse wavevector $\mathbf{p}$. We assume that the generated photon is narrowband, with frequency ω, so that the longitudinal wavenumber can be written as $k(\mathbf{p}) = (\omega^2/c^2 - |\mathbf{p}|^2)^{1/2}$.

Any mode function with an arbitrary amplitude profile can be expanded into spiral harmonic modes, so that it can be written as

$$\Phi(\rho, \varphi) = \sum_{m=-\infty}^{\infty} a_m(\rho) \exp(im\varphi) \quad (2)$$

where $\rho = (p_x^2 + p_y^2)^{1/2}$ and $\varphi = \tan^{-1} p_y/p_x$ are cylindrical coordinates in transverse wavevector space.

Mode functions which are not represented by a pure spiral harmonic mode correspond to photons in a superposition state, with the weights of the quantum superposition dictated by the contribution of the mth angular harmonics [28]. The OAM content of the quantum state is then given by the array $P_m = |C_m|^2$. The value of C_m is given by $C_m = \int \mathrm{d}\rho\, \rho |a_m(\rho)|^2$, where

$$a_m(\rho) = \frac{1}{\sqrt{2\pi}} \int \mathrm{d}\varphi\, \Phi(\rho, \varphi) \exp(-im\varphi). \quad (3)$$

Photons that are described by a superposition of OAM states can be prepared in a variety of ways. Such superpositions can be restricted to a finite number of modes, or it can consist of an infinite, but discrete, number of modes.

Within the paraxial regime of light propagation, any classical beam with an arbitrary amplitude profile can be expanded into Laguerre–Gauss (LG) modes, so that the amplitude A of the electric field at $z = 0$ can be written as

$$A(p_x, p_y, z = 0) = \sum_{m=-\infty}^{\infty} \sum_{p=0}^{\infty} C_{mp} U_{mp}(p_x, p_y) \quad (4)$$

where $C_{mp} = \int \mathrm{d}\mathbf{p}\, A(\mathbf{p}) U_{mp}^*(\mathbf{p})$. The functions U_{mp} are Laguerre–Gauss (LG) modes. The index p is the number of non-axial radial nodes of the mode and the index m, referred to as the winding number, describes the helical structure of the wavefront around a phase dislocation. When the amplitude is a pure LG mode with index m, the mode is an eigenstate of the OAM operator with eigenvalue $m\hbar$.

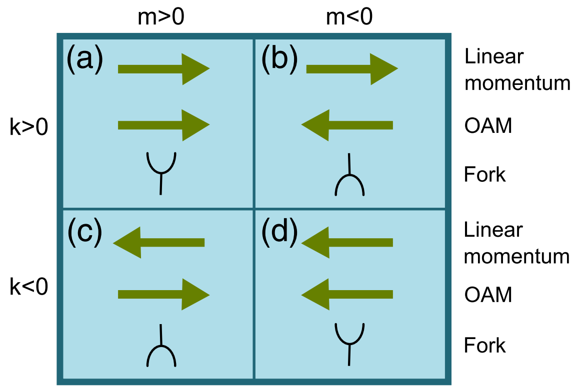

Figure 3. The orbital angular momentum of light. The direction of propagation of the photon determines the direction of the linear momentum vector (**P**). For a photon which is not in a superposition state of spiral harmonic modes (a single index m), the orbital angular momentum operator ($\mathbf{L}_z$) can have the same orientation as the vector (**P**) (this corresponds to an index $m > 0$), or it can have the opposite direction (index $m < 0$). Interference of the OAM-bearing photon with a wide Gaussian beam propagating slightly tilted with respect to the photon will result in a typical fork-like interference pattern that points up or down depending on the sign of the index m.

When we consider photons that propagate in different directions, as will be the case here, there might appear some confusion about how to designate the OAM state of photons. In order to be more specific, let us consider a photon that propagates in the $+\mathbf{z}$ direction, therefore the direction of the linear momentum vector is also $+\mathbf{z}$. If the mode function of the photon is a LG beam with index $m > 0$, the OAM vector L_z has the same direction as the momentum vector, as shown in figure 3(a). If the mode function of the photon is a LG beam with index $m < 0$, the OAM vector has the opposite direction to the linear momentum vector (see figure 3(b)). If the photon reverses its direction of propagation, and therefore its linear momentum, for instance by being reflected in a perfect mirror, the OAM vector does not reverse its direction [29], and the index m that describes mathematically the mode function is still the same as before the photon was reflected, but it is clear that the reflected photon *is different* to the incident photon.

What *is relevant physically is not the sign of m, which depends on the direction of propagation of the photon, but the relationship between the linear momentum and the OAM*, so we can distinguish two types of photons, in relation to its OAM: photons where linear momentum and OAM vectors point out in the same direction, as shown in figures 3(a) and (d); and photons where the linear momentum and OAM vectors show opposite directions (figures 3(b) and (c)). Both types of photons can be easily distinguished by making them interfere with a plane wave that propagates in the same direction, resulting in a pattern of interference with a fork-like structure, inverted or not, depending on the type of photons present.

To avoid any confusion, we will always consider appropriate coordinate systems for each photon, where the $+\mathbf{z}_i$ ($i = 1, 2$) axis is always given by the linear momentum of the photon, therefore by its direction of propagation. In this way, the electric field ($E_{\rm in}$) of the incident photon on the mirror, which propagates along the $\mathbf{z}_1 = \mathbf{z}$ direction, can be written as

$$E_{\rm in}(\mathbf{x}_1, z_1, t) = \int \mathrm{d}\mathbf{p}\, U_{mp}(\mathbf{p}) \exp\left(\mathrm{i}kz_1 + \mathrm{i}\mathbf{p}\cdot\mathbf{x}_1 - \mathrm{i}\omega t\right) \quad (5)$$

while the electric field of the reflected photon ($E_{\rm out}$), which propagates along the direction $\mathbf{z}_2 = -\mathbf{z}$, can be written as

$$E_{\rm out}(\mathbf{x}_2, z_2, t) = \int \mathrm{d}\mathbf{p}\, U_{-mp}(\mathbf{p}) \exp(\mathrm{i}kz_2 + \mathrm{i}\mathbf{p}\cdot\mathbf{x}_2 - \mathrm{i}\omega t). \quad (6)$$

When we write both electric fields in the common coordinate system $(\mathbf{x}, z)$, and we take into account the relationships between the coordinate systems $(\mathbf{x}_1, z_1)$ and $(\mathbf{x}_2, z_2)$, i.e., $x_1 = x_2 = x$ and $y_1 = -y_2 = y$, we obtain

$$E_{\rm in}(\mathbf{x}, z, t) = \int \mathrm{d}\mathbf{p}\, U_{mp}(\mathbf{p}) \exp(\mathrm{i}kz + \mathrm{i}p_x x + \mathrm{i}p_y y - \mathrm{i}\omega t)$$
$$E_{\rm out}(\mathbf{x}, z, t) = \int \mathrm{d}\mathbf{p}\, U_{-mp}(\mathbf{p}) \exp(-\mathrm{i}kz + \mathrm{i}p_x - \mathrm{i}p_y y - \mathrm{i}\omega t) \quad (7)$$

showing explicitly the change of the OAM state (from $+m$ to $-m$).

2.2. Pairs of photons

The quantum state of a two-photon pair is given by

$$|\Psi\rangle = \int \mathrm{d}\mathbf{p}\,\mathrm{d}\mathbf{q}\, \Phi(\mathbf{p}, \mathbf{q}) a_{\rm s}^\dagger(\mathbf{p}) a_{\rm i}^\dagger(\mathbf{q})|0\rangle_{\rm s}|0\rangle_{\rm i} \quad (8)$$

where $\mathbf{p}$ and $\mathbf{q}$ are the transverse components of the signal and idler wavevectors, and $a_{\rm s,i}^\dagger$ are the corresponding creation operators for the signal and idler photons, respectively. One can decompose the mode function in the base of the eigenstates of the OAM operator as [14]

$$\Phi(\mathbf{p}, \mathbf{q}) = \sum_{m_1}\sum_{m_2} C_{m_1}^{m_2}(\rho_1, \rho_2) \exp(-\mathrm{i}m_1\varphi_1 - \mathrm{i}m_2\varphi_2). \quad (9)$$

If the idler photon is projected into the quantum state $|m_2, p_2\rangle_{\rm i}$, whose mode function is a LG beam, the signal photon turns out to be

$$|\Psi_{\rm s}\rangle = \int \mathrm{d}\mathbf{p}\, \Phi_{\rm s}(\mathbf{p}) a_{\rm s}^\dagger(\mathbf{p})|0\rangle_{\rm s} \quad (10)$$

with

$$\Psi_{\rm s}(\mathbf{p}) = \int \mathrm{d}\mathbf{q}\, \Phi(\mathbf{p}, \mathbf{q}) U_{m_2,p_2}^*(\mathbf{q}). \quad (11)$$

The OAM content of the signal photon is given by the corresponding normalized array $P_{m_1} = |C_{m_1}|^2$.

3. What kinds of correlations exist between the OAM of the generated photons?

3.1. SPDC: the full down-conversion cone

Let us consider a nonlinear crystal of length L (from $z = -L/2$ to $z = L/2$), illuminated by a monochromatic laser pump beam propagating in the z direction, with frequency $\omega_{\rm p}$. The spatial shape of the pump beam at the center of the nonlinear crystal ($z = 0$), in the transverse wavevector domain, can be written as $E_{\rm p}(\mathbf{p}) = E_0(p_x + \mathrm{i}p_y)^{m_{\rm p}} \exp(-|\mathbf{p}|^2 w_0^2/4)$, which corresponds to a beam which carries an OAM of $m_{\rm p}\hbar$ per photon. E_0 is a normalization constant, $\mathbf{p} = (p_x, p_y)$ is the transverse wavevector and w_0 is the beam width. The signal and idler photons are assumed to be monochromatic, with $\omega_{\rm s} = \omega_{\rm i} = \omega_{\rm p}/2$, where $\omega_{\rm s,i}$ are the frequencies of the signal and idler photons. This is justified by the use of narrowband interference filters in front of the detectors.

We neglect the effect of the Poynting vector walk-off of the interacting beams. The angle of the down-conversion cone is assumed to be small, so that the polarization [30] and refractive index do not show noticeable changes with the direction of propagation. The nonlinear coefficient is assumed to be constant as well.

If we assume a coherent state for the pump beam, with coherent-state amplitude $\mathcal{E}_{\rm p}$, the effective Hamiltonian in the interaction picture, can be written as

$$H_{\rm I}^{\rm SPDC} = \epsilon_0 \int \mathrm{d}V\, \chi^{(2)} \mathcal{E}_{\rm s}^- \mathcal{E}_{\rm i}^- \mathcal{E}_{\rm p} + \text{h.c.} \quad (12)$$

At first-order perturbation theory, the mode function Φ of the two-photon quantum state is given by,

$$\Phi(\mathbf{P}, \mathbf{Q}) = E_{\rm p}(\mathbf{P} + \mathbf{Q})\mathrm{sinc}(\Delta_k L/2) \quad (13)$$

where $\mathbf{P}$ and $\mathbf{Q}$ are the transverse wavevectors for the signal and the idler. Δ_k is given by $\Delta_k = k_{\rm p}(\mathbf{P}+\mathbf{Q}) - k_{\rm s}(\mathbf{P}) - k_{\rm i}(\mathbf{Q})$, where the wavevectors write $k_j(\mathbf{P}) = [(\omega_j n_j/c)2 - |\mathbf{P}|^2]^{1/2}$ with (j = s, i, p), and n_j are the corresponding refractive index.

We can write $|\mathbf{P} + \mathbf{Q}|^2 = \rho_{\rm s}^2 + \rho_{\rm i}^2 + 2\rho_{\rm s}\rho_{\rm i}\cos(\varphi_{\rm s} - \varphi_{\rm i})$, where $\rho_{\rm s} = |\mathbf{P}|$, and $\varphi_{\rm s} = \tan^{-1} P_y/P_x$ are the modulus and phase of the transverse wavevector $\mathbf{P}$ in cylindrical coordinates. For the idler photon we have, similarly, $\rho_{\rm i} = |\mathbf{Q}|$ and $\varphi_{\rm i} = \tan^{-1} Q_y/Q_x$. Therefore, one can write $\mathrm{sinc}(\Delta_k L/2) = \sum_{l=-\infty}^{\infty} \mathcal{H}_l(\rho_{\rm s}, \rho_{\rm i}) \exp\{\mathrm{i}l(\varphi_{\rm s} - \varphi_{\rm i})\}$. The pump beam can also be written as

$$E_{\rm p}(\mathbf{P} + \mathbf{Q}) = E_0 \exp\left\{-\frac{\left[\rho_{\rm s}^2 + \rho_{\rm i}^2 + 2\rho_{\rm s}\rho_{\rm i}\cos(\varphi_{\rm s} - \varphi_{\rm i})\right] w_0^2}{4}\right\} \times \sum_{l=0}^{m_{\rm p}} \begin{pmatrix} m_{\rm p} \\ l \end{pmatrix} \rho_{\rm s}^l \rho_{\rm i}^{m_{\rm p}-l} \exp\left\{\mathrm{i}l\varphi_{\rm s} + \mathrm{i}\left(m_{\rm p} - l\right)\varphi_{\rm i}\right\}. \quad (14)$$

The mode function given by equation (13) can thus be written as

$$\Phi(\mathbf{P}, \mathbf{Q}) = \sum_{m=-\infty}^{\infty} \mathcal{G}_m(\rho_{\rm s}, \rho_{\rm i}) \exp\left[\mathrm{i}m\varphi_{\rm s} + \mathrm{i}(m_{\rm p} - m)\varphi_{\rm i}\right] \quad (15)$$

where the function $\mathcal{G}$ is determined by equation (14).

The main conclusion to be drawn from equation (15) is that, if polarization, refractive index and nonlinear coefficient show negligible azimuthal variations along the down-conversion cone, the OAM correlations of the spatial waveform of the biphoton state fulfil $m_{\rm p} = m_{\rm s} + m_{\rm i}$ [12]. Importantly, this result requires considering *the whole spatial waveform of the down-converted photons, i.e. the full down-conversion cone*. Notwithstanding, these *are not* the OAM correlations that typical quantum information experiments based on spatial entanglement measure.

3.2. Raman transitions in atomic ensembles: all directions

We assume coherent monochromatic modes for the control and pump beams, with coherent-state amplitudes $\mathcal{E}_c$ and $\mathcal{E}_p$ respectively. For non-resonant pump and control beams, the effective nonlinearity $\chi^{(3)}$ does not depend on the intensity of those beams [31]. The distribution of atoms in the cloud is assumed to be Gaussian, so the effective nonlinearity $\chi^{(3)}$ can be written as

$$\chi^{(3)}(x, y, z) \propto \exp\left[-\frac{x^2+y^2}{R^2} - \frac{z^2}{L^2}\right] \tag{16}$$

where R is the size of the cloud of atoms in the transverse plane (x, y) and L is the size in the longitudinal direction. The generated Stokes and Anti/Stokes photons are narrowband (∼GHz) [20]; thus, the Stokes and anti-Stokes photons are assumed to be monochromatic, with $\omega_p+\omega_c = \omega_s+\omega_{as}$, where $\omega_{s,as}$ are the frequencies of the Stokes and anti-Stokes photons, and $\omega_{p,c}$ correspond to the frequencies of the pump and control beams.

The effective Hamiltonian in the interaction picture, that describes the photon–atom interaction, can be written as

$$H_I = \epsilon_0 \int dV\, \chi^{(3)} \mathcal{E}_{as}^- \mathcal{E}_s^- \mathcal{E}_c \mathcal{E}_p + \text{h.c.} \tag{17}$$

The mode function Φ that describes the quantum state of the generated pair of photons, at first order of perturbation theory, is written as

$$\Phi(\mathbf{Q}_s, \mathbf{Q}_{as}) = \int d\mathbf{Q}_p\, d\mathbf{Q}_c\, E_p(\mathbf{Q}_p) E_c(\mathbf{Q}_c) \times \exp\left(-\Delta_1^2 R^2/4 - \Delta_2^2 R^2/4 - \Delta_0^2 L^2/4\right) \tag{18}$$

where

$$\Delta_1 = Q_p^x + Q_c^x - Q_s^x - Q_{as}^x$$

$$\Delta_2 = Q_p^y - Q_c^y - Q_s^y + Q_{as}^y$$

$$\Delta_0 = k_p - k_c - k_s + k_{as}$$

and the longitudinal wavevector of the any of the interacting beams can be written as $k_i = [(\omega_i n_i/c)^2 - |Q_i|^2]^{1/2}$. n_i is the refractive index at the corresponding wavelength, $|\mathbf{Q}_i|^2 = (Q_i^x)^2 + (Q_i^y)^2$ and c is the velocity of light in vacuum.

Let us define radial ρ_i and azimuthal φ_i coordinates $Q_i^x = \rho_i \cos\varphi_i$ and $Q_i^y = \rho_i \sin\varphi_i$ for i = p, c, s, as. The pump and control beams are written as Laguerre–Gauss beams, $E_p(\rho_p, \varphi_p) \propto \rho_p^{m_p} \exp(-\rho_p^2 w_p^2/4) \exp(i m_p \varphi_p)$ and $E_c(\rho_c, \varphi_c) \propto \rho_c^{m_c} \exp(-\rho_c^2 w_c^2/4) \exp(i m_c \varphi_c)$, where $m_{p,c}$ designate the OAM content of the beams, and $w_{p,c}$ are the corresponding beam waists. $\Delta_0 = k_p(\rho_p) - k_c(\rho_c) - k_s(\rho_s) + k_{as}(\rho_{as})$ depend only on the radial coordinates, and

$$\begin{aligned}\Delta_1^2 + \Delta_2^2 &= \rho_p^2 + \rho_c^2 + \rho_s^2 + \rho_{as}^2 + 2\rho_p\rho_c\cos(\varphi_p+\varphi_c) \\ &\quad - 2\rho_p\rho_s\cos(\varphi_p-\varphi_s) - 2\rho_p\rho_{as}\cos(\varphi_p+\varphi_{as}) \\ &\quad - 2\rho_c\rho_s\cos(\varphi_c+\varphi_s) - 2\rho_c\rho_{as}\cos(\varphi_c-\varphi_{as}) \\ &\quad + 2\rho_s\rho_{as}\cos(\varphi_s+\varphi_{as}).\end{aligned} \tag{19}$$

Equation (18) can thus be written as

$$\Phi(\rho_s, \varphi_s, \rho_{as}, \varphi_{as}) = \sum_{m=-\infty}^{\infty} \mathcal{F}_m(\rho_s, \rho_{as}) \times \exp\left[i m\varphi_s + i(m - m_p + m_c)\varphi_{as}\right] \tag{20}$$

where the function $\mathcal{F}_m$ comes from integrating over ρ_p and ρ_c. The specific signs that appear in equation (20) come from the different directions of propagation of all waves, as explained above [32].

Notice that equation (20) is formally identical to equation (15). Both in the case of SPDC, and in the case of Raman transitions induced in atomic ensembles, the relationships $m_p = m_s + m_i$ and $m_p - m_c = m_s - m_{as}$ describe perfect correlations between the OAM state of each photon of the generated pair. The pump beam in one case, and the pump and control beams in the other case, establish a special direction, the **z** axis. The existence of azimuthal symmetry around this axis is therefore reflected in the existence of perfect OAM correlations between the two photons. But anything that would break such symmetry, would manifest in the violation of such a selection rule. In SPDC configurations, this might be the presence of Poynting vector walk-off of some of the interacting waves [15, 16]. In paired photons generated in atomic ensembles, this might be a noncylindrical distribution of atoms in both transverse dimensions.

4. Orbital angular momentum correlations in collinear configurations

We refer as collinear configurations to those configurations where the generated photons co-propagate or counter-propagate with the pump and control beams that mediate the generation of the photons. In this case, the mode function that describes the spatial shape of the pairs of photons is formally identical to equation (13) for SPDC, or to equation (18) for Raman transitions. Therefore, the selection rules $m_p = m_s + m_i$ (for SPDC) and $m_p - m_c = m_s - m_{as}$ for Raman transitions in atomic ensembles apply as well [27, 32]. But notice that now we are considering paired photons generated in specific directions.

The equivalence does not necessarily apply to the weight of each mode in the corresponding OAM decomposition. Although the selection rules that determine the OAM correlations are the same, the probability of detecting particular OAM modes can change. In [14], it was shown how to engineer such weights for the case of SPDC, by controlling the pump beam width and the length of the nonlinear crystal.

As an example, let us consider a type II noncritical collinear configuration. Such a configuration can be achieved, for instance, using a periodically poled KTP crystal, where all waves propagate along the X axis of the nonlinear crystal, and the generated photons bear orthogonal polarizations. In such a collinear configuration ($\varphi = 0$), the spatial mode function of the biphoton can be written as [33]

$$\Phi(\mathbf{p}, \mathbf{q}) = E_p(\mathbf{p}+\mathbf{q}) \operatorname{sinc}\left[\frac{|\mathbf{p}-\mathbf{q}|^2 L}{4k_p^0}\right] \tag{21}$$

where $k_p^0 = k_p(\mathbf{p} = 0)$. In this case, the relationship $m_p = m_s + m_i$ is fulfilled.

The phase matching function, $\mathrm{sinc}(\Delta_k L/2)$, can be approximated by an exponential function that has the same width at the $1/e^2$ of the intensity: $\mathrm{sinc}(bx^2) \simeq \exp[-\Gamma bx^2]$, with $\Gamma = 0.455$. For the case of a Gaussian pump beam, equation (21) can thus be written as

$$\Phi(\mathbf{p},\mathbf{q}) = \left[\frac{w_0^2 \Gamma L}{\pi^2 k_p^0}\right]^{1/2} \exp\left[-\frac{|\mathbf{p}+\mathbf{q}|\, w_0^2}{4}\right] \times \exp\left[-\frac{\Gamma L}{4k_p^0}|\mathbf{p}-\mathbf{q}|^2\right]. \quad (22)$$

Under these conditions, the OAM decomposition [14] of the mode function given by equation (22) is also the Schmidt decomposition of the mode function [34, 35], and is written as

$$\Phi(\mathbf{p},\mathbf{q}) = \sum_{m,p} C_{mp} U_{mp}(\mathbf{p})\, U_{-mp}(\mathbf{q}) \quad (23)$$

where

$$C_{mp} = (1-z) z^{|m|/2+p} \quad (24)$$

with

$$z = \left[\frac{w_0^2 - \Gamma L/k_p^0}{w_0^2 + \Gamma L/k_p^0}\right]^2 \quad (25)$$

and $\sum_{m=-\infty}^{\infty} \sum_{p=0}^{\infty} |C_{mp}|^2 = 1$. Notice that, under the Gaussian approximation, Schmidt modes are anti-correlated in the index m, but show perfect correlation in the index p. For $w_0 = \sqrt{\Gamma L/k_p^0}$, the pair of photons is not spatially entangled, i.e., only one term of the Schmidt decomposition ($m = 0$ and $p = 0$) remains. This is the appropriate working configuration when the goal is to generate pairs of photons non-entangled, and with a Gaussian shape. For typical values in PPKTP ($\lambda_p = 405$ nm, a crystal length of $L = 30$ mm and refractive index $n_p \sim 1.7$), one obtains $w_0 \sim 22\ \mu$m.

5. Conclusion

When considering all of the possible directions of emission of the generated pairs of photons, the main conclusion to be drawn is that, if there is no source of azimuthal distinguishability with respect to the special direction set-up by the pump and control beams' directions of propagation, the selection rules $m_p = m_s + m_i$ for SPDC, and $m_p - m_c = m_s - m_{as}$ for Raman transitions, are fulfilled. This is also the case for configurations where, although specific directions of emission are considered, the generated photons co-propagate or counter-propagate with the pump and control beams.

On the other hand, we should notice that the question of the total angular momentum conservation balance in SPDC requires the simultaneous consideration of the angular momentum of the electronic spins and orbitals, the crystalline structure of the nonlinear crystal and of the electromagnetic field [36, 37]. The analysis presented here might be an important step towards clarifying how angular momentum is effectively conserved, since to evaluate conservation laws, one should take into account *all probability amplitudes* that contribute to the quantum process.

In general, the azimuthal distinguishing information introduced in non-collinear configurations can affect the quantum properties of the photons generated, and cannot be neglected, even when other degrees of freedom of the photons are considered. This is the case, for instance, when the configurations considered here are used as sources of polarization-entangled photons. The azimuthal distinguishing information introduced by the direction of emission can affect the quantum properties of polarization-entangled photons when these photons are generated with different angles of emission [16]. This is the case when using two type I SPDC crystals whose optical axes are rotated 90°. This configuration, originally demonstrated for the generation of polarization-entangled photons [38, 39], has been used as well for the generation of hyperentangled quantum states [4].

It is also the case of the source considered in [40]. If the volume of interaction is spherical-like ($R \simeq L$), the realization of high-dimensional entanglement by selecting several spatial modes (directions of emission), as proposed in [40], can be achieved without introducing spatial distinguishing information between different pairs of photons [16], which can degrade the quality of the entanglement generated. On the other hand, the presence of ellipticity of the mode function as a function of the emission angle, could restrict the angles of emission accessible for generating a polarization-entangled state with a degree of concurrence above a certain prescribed level.

Acknowledgments

This work was supported by projects FIS2007-60179 and Consolider-Ingenio 2010 QOIT from the Government of Spain, by the European Commission (Qubit Applications (QAP), Contract No. 015848) and by the Generalitat de Catalunya.

References

[1] Molina-Terriza G, Torres J P and Torner L 2007 *Nat. Phys.* **3** 305
[2] Vaziri A, Pan J W, Jennewein T, Weihs G and Zeilinger A 2003 *Phys. Rev. Lett.* **91** 227902
[3] Molina-Terriza G, Vaziri A, Ursin R and Zeilinger A 2005 *Phys. Rev. Lett.* **94** 040501
[4] Barreiro J T, Langford N K, Peters N A and Kwiat P G 2005 *Phys. Rev. Lett.* **95** 260501
[5] Mair A, Vaziri A, Weihs G and Zeilinger A 2001 *Nature* **412** 313
[6] Walborn S P, de Oliveira A N, Thebaldi R S and Monken C H 2004 *Phys. Rev.* A **69** 023811
[7] Molina-Terriza G, Vaziri A, Rehacek J, Hradil Z and Zeilinger A 2004 *Phys. Rev. Lett.* **92** 167903
[8] Langford N K, Dalton R B, Harvey M D, O'Brien J L, Pryde G J, Gilchrist A, Bartlett S D and White A G 2004 *Phys. Rev. Lett.* **93** 053601
[9] Burnham D C and Weinberg D L 1970 *Phys. Rev. Lett.* **25** 84
[10] Altman A R, Koprulu K G, Corndorf E, Kumar P and Barbosa G A 2005 *Phys. Rev. Lett.* **94** 123601
[11] Molina-Terriza G, Minardi S, Deyanova Y, Osorio C Y, Hendrych M and Torres J P 2005 *Phys. Rev.* A **72** 065802
[12] Arnaut H H and Barbosa G 2000 *Phys. Rev. Lett.* **85** 286

[13] Franke-Arnold S, Barnett S M, Padgett M J and Allen L 2002 *Phys. Rev.* A **65** 033823
[14] Torres J P, Alexandrescu A and Torner L 2003 *Phys. Rev.* A **68** 050301
[15] Torres J P, Molina-Terriza G and Torner L 2005 *J. Opt. B: Quantum Semiclass. Opt.* **7** 235
[16] Osorio C I, Molina-Terriza G, Font B and Torres J P 2007 *Opt. Express* **15** 14636
[17] Fedorov M V, Efremov M A, Volkov P A, Moreva E V, Straupe S S and Kulik S P 2008 *Phys. Rev.* A **77** 032336
[18] Duan L M, Cirac J I and Zoller P 2002 *Phys. Rev.* A **66** 023818
[19] Matsukevich D N, Chaneliere T, Bhattacharya M, Lan S Y, Jenkins S D, Kennedy T A B and Kuzmich A 2005 *Phys. Rev. Lett.* **95** 040405
[20] Balic V, Braje D A, Kolchin P, Yin G Y and Harris S E 2005 *Phys. Rev. Lett.* **94** 183601
[21] Inoue R, Kanai N, Yonehara T, Miyamoto Y, Koashi M and Kozuma M 2006 *Phys. Rev.* A **74** 053809
[22] Eberly J H 2006 *J. Phys. B: At. Mol. Opt. Phys.* **39** S599
[23] Scully M O, Fry E S, Ooi C H R and Wodkiewicz K 2006 *Phys. Rev. Lett.* **96** 010501
[24] Kuzmich A, Bown W P, Boozer A D, Boca A, Chou C W, Duan L M and Kimble H J 2003 *Nature* **423** 731
[25] Kolchin P, Du S, Belthangady C, Yin G Y and Harris S E 2006 *Phys. Rev. Lett.* **97** 113602
[26] Chen Q F, Shi B S, Zhang Y S and Guo C G 2008 *Phys. Rev.* A **78** 053810
[27] Osorio C I, Barreiro S, Mitchell M W and Torres J P 2008 *Phys. Rev.* A **78** 052301
[28] Molina-Terriza G, Torres J P and Torner L 2002 *Phys. Rev. Lett.* **88** 013601
[29] Loudon R 2003 *Phys. Rev.* A **68** 013806
[30] Migdall A 1997 *J. Opt. Soc. Am.* B **14** 1093
[31] Braje D A, Balic V, Goda S, Yin G Y and Harris S E 2004 *Phys. Rev. Lett.* **93** 183601
[32] Torres J P, Osorio C I and Torner L 2004 *Opt. Lett.* **29** 1939
[33] Walborn S P, de Oliveira A N, Padua S and Monken C H 2003 *Phys. Rev. Lett.* **90** 143601
[34] Law C K and Eberly J H 2004 *Phys. Rev. Lett.* **92** 127903
[35] Chan K W, Torres J P and Eberly J H 2007 *Phys. Rev.* A **75** 050101
[36] Bloembergen N 1969 Conservation of angular momentum for optical processes in crystals *Polarization, Matiere et Rayonnement* (Paris: Presses Universitaires) p 109
[37] Bloembergen N 1980 *J. Opt. Soc. Am.* B **12** 1429
[38] Kwiat P G, Waks E, White A G, Appelbaum I and Eberhard P H 1999 *Phys. Rev.* A **60** R773
[39] Altepeter J, Jeffrey E and Kwiat P 2005 *Opt. Express* **13** 8951
[40] Chen S, Chen Y A, Zhao B, Yuan Z S, Schmiedmayer J and Pan J W 2007 *Phys. Rev. Lett.* **99** 180505